

## Effect of Clay/Diamond and Clay/Carbon Nanosystems on Structure-Properties Relationships of iPP

Clara Silvestre,<sup>\*1</sup> Sossio Cimmino,<sup>1</sup> Maria Raimo,<sup>1</sup> Cosimo Carfagna,<sup>1</sup> Vincenzo Capuano,<sup>1</sup> Rumiana Kotsilkova<sup>2</sup>

<sup>1</sup>Istituto di Chimica e Tecnologia dei Polimeri. CNR. Via Campi Flegrei, 34 80078 - Pozzuoli (Naples), Italy

E-mail: silv@irtemp.na.cnr.it

<sup>2</sup>Central Laboratory of Physico-Chemical Mechanics, Bulgarian Academy of Sciences, Acad. G. Bonchev Str., Block 1, 1113 Sofia, Bulgaria

**Summary:** The effect of the addition of two combined fillers, smectite clay and diamond and smectite clay and carbon nanoparticles, on structure, morphology, isothermal and non isothermal crystallization behaviour, tensile and thermal properties of isotactic polypropylene (iPP) has been investigated by using several techniques: wide angle X-ray diffraction, optical and scanning electron microscopy, thermogravimetry, differential scanning calorimetry and tensile techniques. It was found that nanoparticles of diamond and carbon favour the nucleation of the  $\beta$ -form of iPP crystal, whereas the clay nanolayers do not have any influence on the crystal structure of iPP. The thermal stability of iPP/(clay+diamond) and iPP/(clay+carbon) is improved with respect to neat iPP, whereas no influence is detected when only clay is added to iPP. At the given crystallization conditions, the overall crystallization peak of iPP/(clay+diamond) almost exactly overlaps the crystallization peak of neat iPP, whereas in the case of iPP/clay and iPP/(clay+carbon) the maximum of the crystallization peaks is shifted to higher temperature. The spherulite growth rate,  $G$  values do not differ from one another. The iPP/(clay+carbon) system shows ductile behavior. The other systems show brittle behavior with failure before necking. These results were related with the very high percentage of beta phase present in the samples of iPP/(clay+carbon).

**Keywords:** carbon; diamond; nanocomposites; poly(propylene); properties; structure

### Introduction

Polymers blended with inorganic nanoparticles are an emerging class of filled plastics. Due to the nanosize dimensions of the fillers, their large surface area and specific interfacial

effects, nanocomposites are expected to present unusual properties when compared with pure polymers or conventional microscopic composites.<sup>[1,2]</sup> The most used fillers are silicate nanocomposites, (clay). A large number of polymers have been used as polymeric matrix for polymer/clay nanocomposites, for applications in packaging, automotive components, electrical/electronic parts, building and construction products. These nanocomposites, in fact, have shown significantly enhanced mechanical and thermal properties, improved barrier performance and flame retardancy. Despite of the superior properties reported, many difficulties appear when manufacturing nanocomposite materials.<sup>[3,4]</sup>

Not all polymers are equally well-suited for nanocomposite development. In particular polypropylene/clay nanocomposites are relatively difficult to obtain, because iPP does not contain any polar group in its backbone and it is not compatible with clay. On the other hand polypropylene is one of the most important commodity polymers with a broad range of applications.<sup>[5, 6]</sup> In order to increase the use of iPP in the fields where this polymer presents some limitations (due for examples to the high flammability, the low stiffness at high temperature or the not elevated barrier properties) numerous studies are still in progress: one of the route is that to modify the iPP by adding appropriate fillers. The majority of the results were summarized in the extensive review by Ray and Okamoto recently appeared.<sup>[4]</sup> Beside clay, other nanofillers for polypropylene are under investigation. They include carbon nanoparticles and diamond nanoparticles which have been successfully produced semi-industrially by the Bulgarian Academy of Sciences.<sup>[7]</sup> Nanoscale diamond particles are expected to be promising fillers in respect to the tribotechnical properties, adhesion and corrosion resistance. All these performance benefits could be available without increasing the density or reducing the light transmission properties of the base polymer.

In previous studies<sup>[8-10]</sup> on epoxy/clay and PMMA/clay hybrids, it was found that the presence of clay nanolayers and the interfacial effects suppress significantly the overall molecular dynamics. Rheology-structure relationship has been discussed as a tool for

optimization of formulation, processing and specific properties. Nanosized carbon particles, produced by shock wave technology, offer new opportunities to modify physical properties of insulating polymer matrices. In particular, rheology, conductivity and microwave properties of thermosetting polymer composites containing nanosized carbon particles have been investigated and a good correlation among the three characteristics was found<sup>[10,11]</sup>. In this paper, a study of the reinforcement effects of two combined fillers, smectite clay and diamond and smectite clay and carbon nanoparticles, on structure, morphology, crystallization behavior and tensile and thermal properties of iPP will be reported.

In particular an iPP suitable for fiber production is used with the final aim to obtain a polypropylene/nanocomposite material with improved flammability for textiles. The study of interactions between the fillers together with the results of flammability tests and fiber properties will be reported in a forthcoming paper.

## Experimental

### *Materials and samples preparation*

The polypropylene used in this work is a commercial product, Moplen S30S (kindly provided by Basell, Ferrara, Italy), suitable to be extruded in form of fibers with a melt flow index of 1.8 (g/10min). Smectite clay (SAN), organically modified with quarternized ammonium salt, was used, supplied by CO-OP Chemical, Japan. Diamond and carbon nanoparticles, a few nanometers of diameter, were obtained by decomposition of appropriate explosives as a result of a detonation process (shock wave technology) and supplied by the Bulgarian Academy of Sciences.<sup>[17]</sup> In order to improve the compatibility of iPP with clay and diamond/carbon nanoparticles, hybrid systems were preliminary prepared by nano-level dispersing of filler in an epoxy resin matrix, and, further on, introduced as a swelling agent in iPP. Three hybrid systems were prepared: 1) epoxy hybrid containing 50 wt % modified smectite clay nanolayers, (this system will be called clay); 2) epoxy hybrid containing a mixture of 48 wt% smectite clay and 2 wt% nanoparticles of diamond, (this

system will be called (clay+diamond)); 3) epoxy hybrid containing a mixture of 48 wt% smectite clay and 2 wt% nanoparticles of carbon, (this system will be called (clay+carbon)).

The liquid nanocomposite hybrid systems containing smectite clay were prepared by intercalation of epoxy matrix (Bisphenol A epoxy resin) within the clay galleries. Details of the preparation are reported in references 8, 9 and 10.

The blends of iPP containing 5 wt% of epoxy nanocomposite systems were prepared by melt mixing in a Brabender-like apparatus at 483 K and 32 rpm for 600s. Thus, the final polypropylene composite blends contain of about 2.5 wt% smectite clay and of 0.1 wt% diamond/or carbon, respectively.

The materials were compression moulded in a press at 473 K for 300 s to allow complete melting without pressure. Then a pressure of 50 bar was applied for 300s. Then the samples were cooled to room temperature with a water-cooling serpentine system present inside the plates of the press. Finally the pressure was released and the mould containing 0.12x6x12cm sheet was removed from the press. Dumbbell-shape specimens for tensile tests were cut from the sheets and used for mechanical tensile measurements according to ASTM D256 standards. Stress-strain curves were obtained by an Instron machine (model 1122) at room temperature and a cross-head speed,  $V_t$ , of 0.017 cm/s, gage length equal to 2.2 cm and nominal strain rate of  $0.0075 \text{ s}^{-1}$ . Modulus, stress and elongation at yield and at rupture were calculated from such curves on an average of 12 specimens.

## **Procedures and Techniques**

### *Structural and morphological analysis*

Wide-angle X-ray diffraction was carried out by using a Philips diffractometer (PW 1050) operating at the  $\text{CuK}_\alpha$  radiation. Measurements of diffracted intensity were made in the angular range of  $3\text{--}45^\circ (2\theta)$ , at room temperature and a scan rate of  $0.017^\circ/\text{s}$ .

Optical analysis and measurements were made with an Axioskop polarizing microscope (Zeiss, Thornwood, NY) equipped with a THMS 600 hot stage (Linkam Scientific Instruments Ltd., UK) and a Linkam TMS91 temperature control unit. Samples for optical

microscopy were prepared by squeezing a small quantity of the material onto a glass cover slip. SEM analysis was performed with a Philips 501 SEM (Philips, The Netherlands) after vacuum metallization of the samples by means of a Polaron sputtering apparatus with Au-Pd alloy. Specimens for scanning electron microscopy (SEM) analysis were dynamically crystallized in the DSC apparatus with the following thermal protocol: 1. heating to 473 K at a scan rate of 0.17 K/s, 2. holding at 473 K for 600 s. 3. cooling to 303 K at a scan rate of -0.17 K/s.

### *Thermal analysis*

The thermal stability of samples was measured using a TC10 Mettler instrument, equipped with an M3 analytical thermobalance (Mettler-Toledo Inc., Columbus, OH). Each sample was heated from 313 to 473 K at a scan rate of 0.083 K/s in air. Calorimetric properties analysis and non isothermal overall crystallization were obtained by using a Mettler TA-3000 differential scanning calorimeter equipped with a control and programming unit and a calorimetric cell. Values of the glass transition temperatures ( $T_g$ ), melting temperature, ( $T_m$ ), crystallinity index,  $X_c$ , were determined by heating samples at 0.33 K/s from 223 K to 476 K. The crystallinity index was calculated by dividing the fusion enthalpy for the theoretical value of 209 J/g for the enthalpy of fusion of 100% crystalline polypropylene.<sup>[12]</sup>

### *Kinetics of crystallization*

Spherulite growth rate and overall crystallization rate were obtained in isothermal and non isothermal conditions by using optical microscopy and differential scanning calorimetry.

Isothermal spherulite growth rate of specimens was carried out under nitrogen by heating from 303 to 473 K at a rate of 0.33 K/s, holding at 473 K for 600 s, then cooling to the selected temperatures (namely 407 and 409 K) at a scan rate of -0.83 K/s. The specimens were held at the crystallization temperature until the occurrence of spherulites impingement. The radius of spherulites was measured with the software Image Pro Plus 3.0 by taking photos at appropriate intervals of time, using a JVC TK-1085E videocamera. The

spherulite growth rate was taken as the slope of the straight lines obtained by plotting the radius as a function of time.

In non-isothermal crystallization the specimens were kept at 473 K for 600 s, then cooled to 413 K and allowed to partially crystallize at that temperature for 240 s in order to observe small spherulites. Finally the temperature was gradually decreased with a cooling rate of -0.033 K/s while images were recorded to obtain the radius of spherulites as function of the temperature, admitting a linear relationship between temperature and time:  $T = -0.033t + 413$ . The derivative  $dr/dT$  of the curve  $r(T)$  was calculated and  $G(T) = dr/dt$  obtained as the product of  $-dr/dT$  for the cooling rate  $dT/dt$ .

Non isothermal crystallization of samples was performed at two different cooling rates (namely -0.033 K/s and -0.17 K/s) by cooling from melt.

## Results and discussion

### *Structure and Morphology*

Isotactic polypropylene, iPP, is a material with several crystal modifications.<sup>[13-16]</sup> The different polymorphs are distinct for the different chain packing geometries of the helices. The appearance of these structures is critically dependent upon crystallization condition and pressure.

The WAXS profiles of all the samples obtained by compression molding are reported in figure 1. The pure iPP and the iPP/clay system present the characteristics profile of the  $\alpha$ -form. For the iPP/(clay+carbon) and iPP/(clay+diamond) systems a mixture of  $\alpha$  and  $\beta$  crystals of polypropylene is generated. In fact the characteristic peaks of the two forms - between 18-19°, corresponding to the (130) plane of the  $\alpha$  phase, and between 15.5- 16.5°, corresponding to the (200) of the  $\beta$  plane, are present. An approximate  $\beta/\alpha$  ratio could be calculated as the ratio between the heights of the two peaks: this approximate procedure gives a value of 35% and 45%  $\beta$  phase for the iPP/(clay+diamond) and iPP/(clay+carbon) sample respectively.

This result indicates that nanoparticles of diamond and carbon favour nucleation of the  $\beta$ -form of iPP crystal, acting as nucleating agents, whereas clay nanolayers do not have any influence on the crystal structure of iPP. Moreover it seems that the  $\beta$ -nucleation effect is more marked when carbon nanoparticles are present.

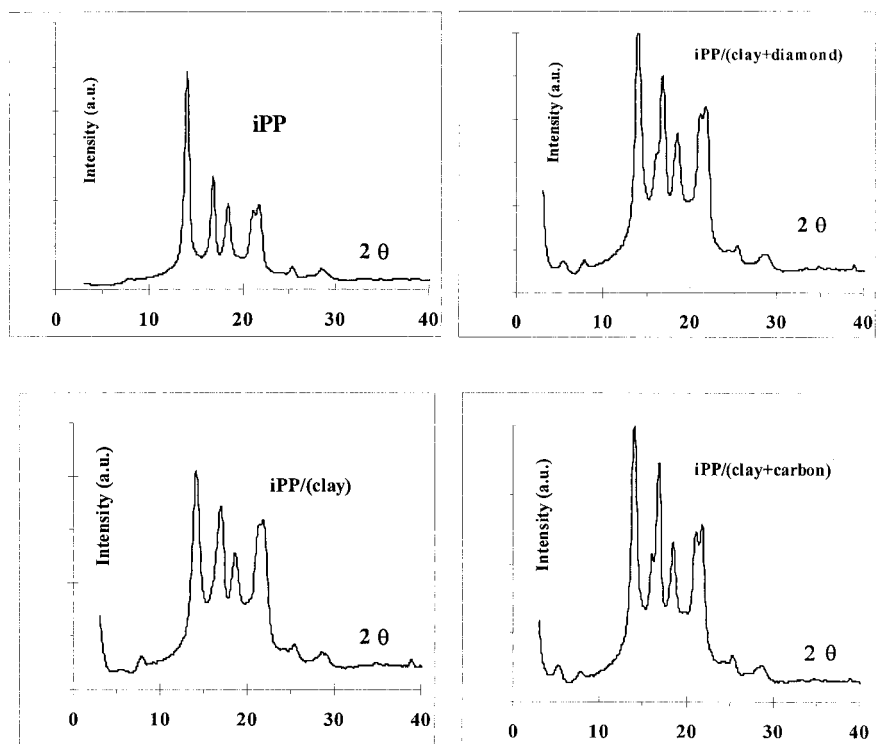
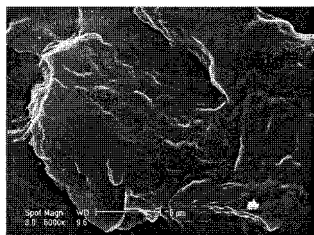


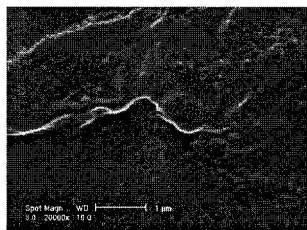
Figure 1. X-ray profiles for iPP and iPP/nanoparticles systems. The intensity is in arbitrary units (a.u.).

Moreover the WAXS patterns offer also a way to determine the interlayer spacing of the silicate layers in the nanocomposites. The appearance of the basal reflection at  $2\theta = 5^\circ$  could indicate the expansion of the clay layers associated with intercalation.

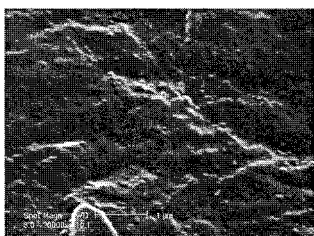
Fractured surfaces of compression molded samples were analyzed by SEM.



(a) iPP/clay



(b) iPP/(clay+diamond)



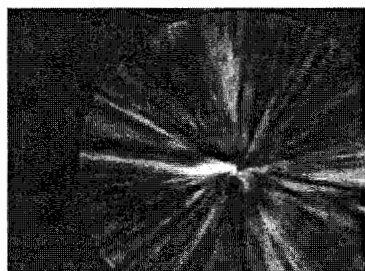
(c) iPP/(clay+carbon)

Figure 2. SEM micrographs of fracture surfaces of the samples as obtained by compression molding, at high magnification.

The micrographs of iPP and iPP/clay show homogeneous surfaces. The surfaces of iPP/(clay+diamond) and iPP/(clay+carbon) present instead small domains homogeneously distributed. For both samples the distribution of the domain size is very narrow. The sizes of the domains depend on the type of nanoparticles. For the iPP/(clay+diamond) samples the dimension of the domains is about 50 nm, whereas it is about 100 nm for the iPP/(clay+carbon) sample. The morphology during isothermal and non-isothermal crystallization from the melt at the selected cooling rate is always spherulitic (see Figure 3). For pure iPP and iPP/clay, the spherulites present generally weak birefringence. Few negative highly birefringence spherulites ( $\beta$ -spherulites) are very sporadically detected. For



the iPP/(clay+diamond) and iPP/(clay+carbon) systems,  $\beta$ -spherulites are frequently detected, in agreement with the X-ray results. At the end of the crystallization process, for all the nanocomposite systems under investigation, larger spherulites than those observed for pure iPP are obtained, for a given crystallization procedure, as shown in Figure 4.

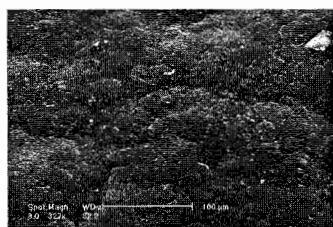


(a) iPP

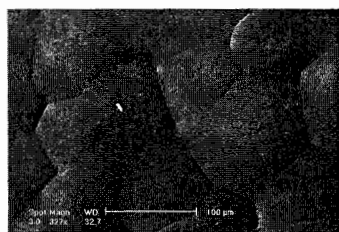


(b) iPP/(clay+diamond);

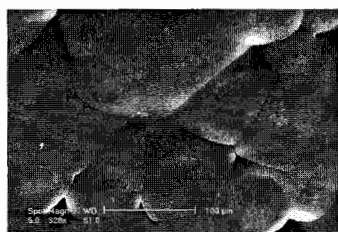
Figure 3. Optical micrographs with crossed polars of iPP spherulites in: (a) iPP; (b) iPP/(clay+diamond).



(a)



(b)



(c)

Figure 4. SEM micrographs of samples crystallized by cooling from melt at  $-0.17$  K/s at low magnification (a) iPP; (b) iPP/clay; (c) iPP/(clay+diamond);

### Thermal analysis

The melting temperature  $T_m$  and the crystallinity level,  $X_c$ , are shown in Table 1. Comparing data reported in Table 1, it emerges that the melting temperature of samples, and the crystallinity content of samples crystallized under the same cooling rate do not significantly change.

Table 1. Melting temperatures,  $T_m$  (K) and crystallinity index,  $X_c$ , of neat iPP iPP/nanosystems for the two scan rates investigated.

Sample	Scan rate [K/s]	$T_m$ [K]	$X_c$ [%]
iPP	0.17	435	50
iPP/clay	0.17	437	50
iPP/(clay+diamond)	0.17	438	51
iPP/(clay+carbon)	0.17	437	53
iPP	0.033	436	56
iPP/clay	0.033	437	54
iPP/(clay+diamond)	0.033	436	53
iPP/(clay+carbon)	0.033	437	56

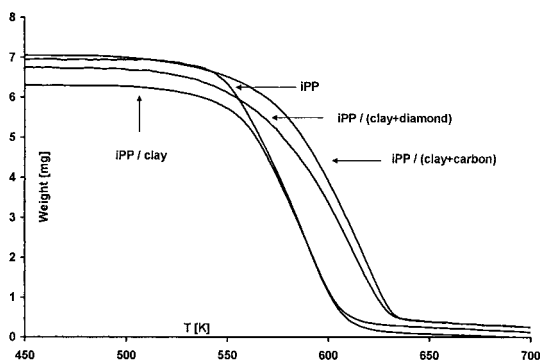


Figure 5. Weight as function of temperature for nanocomposites.

As shown in figure 5 the thermal stability of iPP/(clay+diamond) and iPP/(clay+carbon) in air atmosphere is improved with respect to neat polypropylene, whereas no influence on thermal stability is detected when only clay is added to iPP. Indeed, the iPP/(clay+diamond) and iPP/(clay+carbon) nanocomposites become to lose weight at almost the same temperature of iPP, then the proceeding loss of weight is slowed down and occurs at temperature tens of degrees higher than that of polypropylene. In Table 2 the temperature corresponding to the inflection point of the curves is reported. As the thermogravimetric analysis shows that the decomposition temperature of iPP/clay is slightly affected by the presence of the clay, the higher stability of iPP/(clay+diamond) and iPP/(clay+carbon) has to be due to the presence of nanoparticles of diamond and carbon respectively. This increased thermal stability could be attributed to a slower diffusion of volatile decomposition products within the nanocomposites containing diamond and carbon, suggesting also the hypothesis that these systems could present higher barrier properties, as observed for other polymer nanocomposites.<sup>[4, 8, 17]</sup> Studies are in progress to verify such a hypothesis.

Table 2. Inflection points of termogravimetric curves of samples.

Sample	Inflection temperature [K]
iPP	589
iPP/clay	592
iPP/(clay+diamond)	611
iPP/(clay+carbon)	618

### Crystallization behaviour

In figure 6 the spherulite radial growth rate,  $G$ , as function of the temperature is reported for the nanocomposites, showing that the values do not differ one from another, being their difference within the experimental error. The overall crystallization kinetics of the nanocomposites was studied crystallizing dynamically specimens at two different cooling rates: 0.033 and 0.17 K/min.

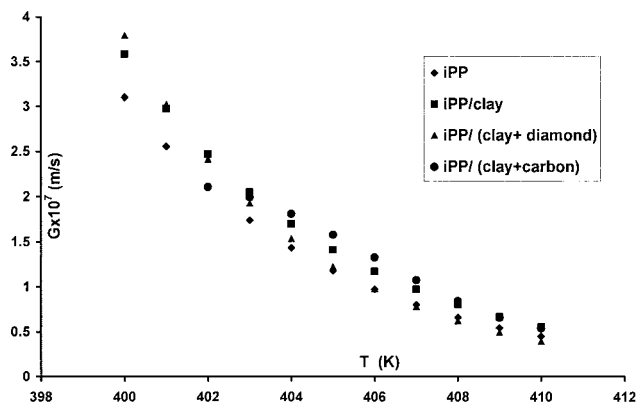


Figure 6. Spherulite radial growth rate of nanocomposites calculated by non-isothermal procedures.

Table 3. Onset and maximum of the crystallization peak of iPP and iPP/nanosystems for the two scan rates investigated.

Sample	Scan rate [K/s]	Onset of the crystallization peak [K] ( $\pm 1$ K)	Maximum of the crystallization peak [K] ( $\pm 1$ K)
iPP	0.17	397	385
iPP/clay	"	399	388
iPP/(clay + diamond)	"	397	385
iPP/(clay + carbon)	"	400	388
iPP	0.033	403	393
iPP/clay	"	405	396
iPP/(clay + diamond)	"	402	393
iPP/(clay + carbon)	"	407	398

In Table 3 the onset (taken as the beginning of the heat evolution) and the maximum of the exothermal crystallization peaks of the nanocomposites are reported. It was found that, at a given cooling rate, the crystallization peak of iPP/(clay+diamond) almost exactly overlaps the crystallization peak of neat iPP, whereas in the case of iPP/clay and iPP/(clay+carbon) the maximum of the crystallization peaks is shifted to higher temperature with a simultaneous change of the onset of the peaks. For example in figure 7 the crystallization peaks of iPP/(clay+carbon) and neat iPP are compared.

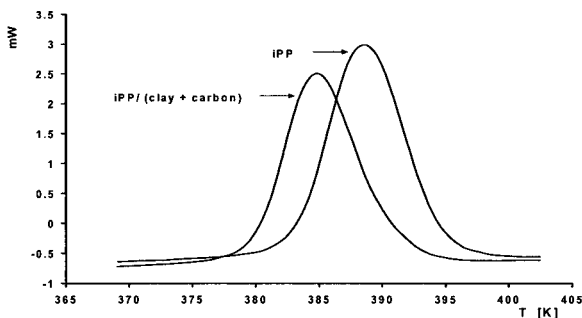


Figure 7. Crystallization peaks of iPP and iPP/(clay + carbon) obtained by cooling from melt at  $-0.17\text{ K/s}$ .

The higher rate of crystallization of iPP/clay and iPP/(clay+carbon) might be in theory due to a higher nucleation rate and/or to higher growth rate of iPP spherulites. But the results presented in the previous sections lead to exclude this hypothesis. In fact the linear growth rate of spherulites is not affected by the presence of nanoparticles and the spherulites of nanocomposites are larger than those observed in neat iPP, showing therefore a minor nucleation density.

Morphological analysis and spherulite growth rate measurements indicate that the higher crystallization rate of iPP/clay and iPP/(clay+carbon) could not be due to higher nucleation density and/or to higher linear growth rate of spherulites. It is difficult to explain this

result with the data in our hand. Work is in progress analyzing different compositions and crystallization conditions.

### *Tensile properties*

Nominal stress-strain curves of the samples of iPP/nanoparticles blends tested at room temperature are presented in figures 8. The neat iPP exhibits yielding point followed by necking, full cold-drawing and fiber rupture, a classical behavior of semicrystalline polymers at room temperature. The behaviors of the blends are dependent on the kind of nanocomposite system added.

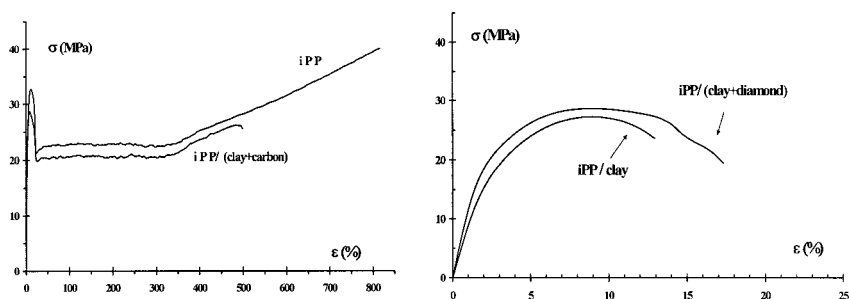


Figure 8. Stress- strain curves.

The iPP/(clay+carbon) blend shows ductile behavior, yielding and cold-drawing phenomena, and formation of the fiber. The other systems show brittle behavior with failure before necking.

The values of the Young's modulus ( $E$ ) of the modified iPP are always higher than that of pure iPP. In the case of iPP/(clay+carbon) this increase reaches the 25%. The ultimate properties ( $\sigma_u$  and  $\epsilon_u$ ) of iPP are strongly influenced by the presence of the nanocomposite. The values of  $\sigma_u$  and  $\epsilon_u$  of the blends decrease in comparison with pure iPP. This result can be related with the very high percentage of beta phase present in the samples iPP/(clay+carbon). It

was in fact reported that in iPP the presence of beta-form within the crystalline portion is beneficial to toughness and ductility of the polymer. <sup>[18, 19]</sup>

## Conclusion

The results reported in this paper show that the addition of two combined fillers, smectite clay and diamond and smectite clay and carbon nanoparticles, to iPP causes drastic modifications in the structure, morphology, tensile and thermal properties of iPP. The principal finding of the paper is the dependence of the crystalline structure and morphology of iPP on the kind of added fillers. In particular it was found that diamond and carbon nanoparticles favour the nucleation of  $\beta$ -form of iPP crystal, whereas clay nanolayers do not have any influence on the crystal structure of iPP.

Several other interesting results were obtained and are worth to be underlined:

- The thermal stability of iPP/(clay+diamond) and iPP/(clay+carbon) is improved with respect to neat iPP and iPP/clay;
- At the given crystallization conditions, the overall crystallization peak of iPP/(clay+diamond) almost exactly overlaps that of iPP. For iPP/clay and iPP/(clay+carbon) the crystallization peaks are shifted to higher temperature;
- The iPP/(clay+carbon) system shows ductile behavior, yielding, cold-drawing phenomena, and formation of the fiber. The other systems show brittle behavior with failure before necking.

## Acknowledgements

This work is supported by the project under the program for scientific cooperation between BAS-Bulgaria and CNR-Italy and by the project CRDC Tecnologie della Regione Campania.

- [1] E. Giannelis, *Advanced Mat.* **1996**, *8*, 29.
- [2] R. Krishnamoorti, E. Giannelis, *Macromolecules* **1997**, *30*, 4097.
- [3] T. Pinnavaia, *Polymer-Clay Nanocomposites*, **2002**.
- [4] S. Sinha Ray, M. Okamoto, *Progress Polymer Science* **2003**, *28*, 1539.
- [5] Macplas, **1998**, *5*, 75.
- [6] Polypropylene to 2004 - Market Size, Market Share, Demand Forecast and Sales (2000) Freedonia grouped.
- [7] S. Stavrev et al. (1994) Method for producing of ultra-dispersed diamond. US Patent No. 5353708.
- [8] R. Kotsilkova, V. Petkova, J. Pelovski, *Journal of Thermal Analysis and Calorimetry* **2001**, *64*, 591.
- [9] A. Kanapitsas, P. Pissis, R. Kotsilkova, *J. Non-Crystal Solids* **2002**, *305*, 204.
- [10] R. Kotsilkova, *Mechanics of Time Dependent Materials*, Kluwer Academic Publisher, **2002**, *6*, 283.
- [11] R. Kotsilkova, D. Nesheva, I. Nedkov, E. Krusteva, S. Stavrev, *J. Appl. Polym. Sci.* **2003**, *92* (4), 2220.
- [12] S.L. Aggarwal, in "Polymer Handbook", 2<sup>nd</sup> ed., J. Brandup, E.H. Immergut, Eds., J.Wiley & Sons, New York 1975, V-24.
- [13] S. Bruckner, S. V. Meille, V. Petraccone, B. Pirozzi, *Progr. Polym. Sci.*, **1991**, *16*, 361.
- [14] J. Varga, "Polypropylene Structure: Blends and Composites Vol.1 Structure and Morphology", J. Karger-Kocsis eds., Chapman and Hall London 1995.
- [15] C. Silvestre, S. Cimmino, E. Di Pace, "Morphology of Polyolefins" *Handbook of Polyolefins: Second Edition, Revised and Expanded* C. Vasile ed. Marcell Dekker New York 2000, chapter 7 175-205.
- [16] A. Phillips, M.D. Wolkowicz, "Polypropylene Handbook, Moore, E.P. Jr. ed., Hanser Publishers Munich Vienna 1996.
- [17] S. J. Ahmadi, Y. D. Huang, W. Li, *J. Mat. Sci.* **2004**, *39*, 1919.
- [18] J. Karger-Kocsis, J. Varga, G. W. Ehrenstein, *J. Appl. Polym. Sci.*, **1997**, *64*, 2057.
- [19] J. Kotex, M. Raab, J. Baldrian, W. Grellmann, *J. Appl. Polym. Sci.*, **2002**, *85*, 1174.